

Density Functional Study of the σ and π Bond Activation at the Pd=X (X = Sn, Si, C) Bonds of the (H₂PC₂H₄PH₂)Pd=XH₂ Complexes. Is the Bond Cleavage Homolytic or Heterolytic?

Toshiaki Matsubara* and Kazuyuki Hirao

Contribution from the Institute for Fundamental Chemistry, 34-4 Takano-Nishihiraki-cho, Sakyo-ku, Kyoto 606-8103, Japan

Received June 1, 2001. Revised Manuscript Received August 27, 2001

Abstract: The mechanism for the activation of the σ bonds, the O–H of H₂O, C–H of CH₄, and the H–H of H₂, and the π bonds, the C≡C of C₂H₂, C=C of C₂H₄, and the C=O of HCHO, at the Pd=X (X = Sn, Si, C) bonds of the model complexes (H₂PC₂H₄PH₂)Pd=XH₂ **5** has been theoretically investigated using a density functional method (B3LYP). The reaction is significantly affected by the electronic nature of the Pd=X bond, and the mechanism is changed depending on the atom X. The activation of the O–H bond with the lone pair electron is heterolytic at the Pd=X (X = Sn, Si) bonds, while it is homolytic at the Pd=C bond. The C–H and H–H bonds without the lone pair electron are also heterolytically activated at the Pd=X bonds independent of the atom X, where the hydrogen is extracted as a proton by the Pd atom in the case of X = Sn, Si and by the C atom in the case of X=C because the nucleophile is switched between the Pd and X atoms depending on the atom X. In contrast, the π bond activation of C≡C and C=C at the Pd=Sn bond proceeds homolytically, and is accompanied by the rotation of the (H₂PC₂H₄PH₂)Pd group around the Pd–Sn axis to successfully complete the reaction by both the electron donation from the π orbital to Sn p orbital and the back-donation from the Pd d π orbital to the π^* orbital. On the other hand, the activation of the C=O π bond with the lone pair electron at the Pd=Sn bond has two reaction pathways: one is homolytic with the rotation of the (H₂PC₂H₄PH₂)Pd group and the other is heterolytic without the rotation. The role of the ligands controlling the activation mechanism, which is heterolytic or homolytic, is discussed.

1. Introduction

The activation of the σ bonds of inert molecules such as H₂, CH₄, and C₂H₆, i.e., H–H, C–H, and C–C, which is an important elementary reaction for organic synthesis, has been a challenging subject for organic chemists. Since the transition metal complexes, which promote these activation reactions under mild experimental conditions, were found about 20–25 years ago, this field has been successfully explored based on tremendous investigations from both experimental¹ and theoretical points of view.²

Recently, Pörschke and co-workers experimentally reported the unique O–H bond activation at the Pd=Sn bond of the phosphine-coordinated palladium complexes. The O–H bond

of water and methanol is easily broken at the Pd=Sn bond of the (R₂PC₂H₄PR₂)Pd=SnR'₂ **5'** (R = *i*-Pr, *t*-Bu; R' = CH–(SiMe₃)₂) complexes³ even at –40 °C to form the (R₂PC₂H₄PR₂)Pd(H)Sn(OR'')R'₂ **7'** (R'' = H, Me) products within a few minutes as given by path i in Figure 1. The water O–H bond can also be independently activated at the Sn of the free stannylene SnR'₂ along another path (ii), which is followed by the Sn–H cleavage at the Pd of the (R'₂PC₂H₄PR'₂)Pd fragment to form complex **7'**.⁴ As this reaction proceeds at more than –10 °C, it suggests that path i is more facile than path ii.

Meanwhile, the transition metal–tin complex has attracted much attention from many chemists because of their unique properties and activities for the synthesis of organic compounds.^{5,6} For example, it is known that the Pd=Sn complexes function as a catalyst for the synthesis of the electrochemically important material stannole. The stannole is catalytically produced by a [2 + 2 + 1] cycloaddition reaction of two ethynes and one stannylene, SnR'₂ (R' = CH(SiMe₃)₂ and R'₂ = {C(SiMe₃)₂CH₂})₂, with the phosphine-coordinated Pd com-

- (1) For example, see: (a) Muetterties, E. L.; Rhodin, T. N.; Band, E.; Brucker, C. F.; Pretzer, W. R. *Chem. Rev.* **1979**, *79*, 91. (b) Shilov, A. E. *The Activation of Saturated Hydrocarbons by Transition Metal Complexes*; D. Reidel: Dordrecht, 1984. (c) Crabtree, R. H. *Chem. Rev.* **1985**, *85*, 245. (d) Cotton, F. A.; Wilkinson, G. In *Advanced Inorganic Chemistry*, 5th ed.; John Wiley & Sons: New York, 1988. (e) Crabtree, R. H. In *The Organometallic Chemistry of the Transition Metals*, 2nd ed.; John Wiley & Sons: New York, 1994.
- (2) For example, see: (a) Koga, N.; Morokuma, K. *Chem. Rev.* **1991**, *91*, 823. (b) Hay, P. J. In *Transition Metal Hydrides*; Dedieu, A., Ed.; VCH: New York, 1992. (c) Siegbahn, P. E. M.; Blomberg, M. R. A. In *Theoretical Aspects of Homogeneous Catalysis*; van Leeuwen, P. W. N. M., Morokuma, K., van Lenthe, J. H., Eds.; Kluwer Academic Publishers: Dordrecht, 1995. (d) Musaev, D. G.; Morokuma, K. In *Advances in Chemical Physics*; Prigogine, I., Rice, S. A., Eds.; John Wiley & Sons: New York, 1996; Vol. XCV.

- (3) Schager, F.; Seevogel, K.; Pörschke, K.-R.; Kessler, M.; Krüger, C. *J. Am. Chem. Soc.* **1996**, *118*, 13075.
- (4) Schager, F.; Goddard, R.; Seevogel, K.; Pörschke, K.-R. *Organometallics* **1998**, *17*, 1546.
- (5) Abel, E. W. *Comprehensive Inorganic Chemistry*; Pergamon Press: Oxford, 1973; Vol. 2, p 43.
- (6) Holt, M. S.; Wilson, W. L.; Nelson, J. H. *Chem. Rev.* **1989**, *89*, 11.

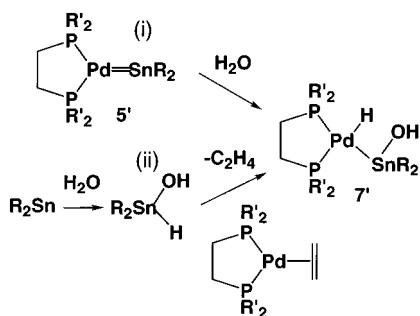
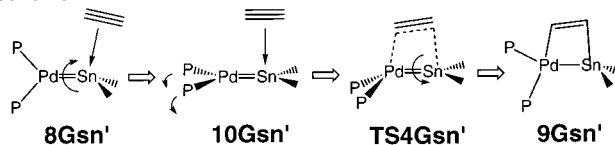


Figure 1. Activation of the water O–H bond at the Pd=Sn bond of the $(R'_2PC_2H_4PR'_2)Pd=SnR_2$ complex (path i) and at the Sn of the free SnR_2 , which is followed by the Sn–H activation at the Pd of the $(R'_2PC_2H_4-PR'_2)Pd$ fragment to form the $(R'_2PC_2H_4PR'_2)Pd(H)Sn(OH)R_2$ complex (path ii).

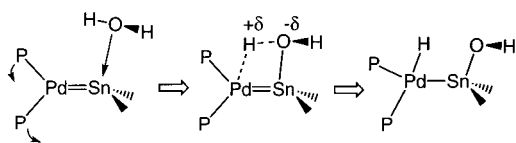
Scheme 1



plexes $(PR_3)_2Pd$ and $(R_2PC_2H_4PR_2)Pd$ ($R = Me, i-Pr, t-Bu$).⁷ In a previous paper, we theoretically clarified by using the density functional method that in the first process of the formation of the 1,2-metallastannete intermediate, $(PR_3)_2Pd-(CH=CH)SnR'_2$ (M–Sn), the activation of the ethyne $C\equiv C$ π bond at the Pd=Sn bond takes place after the formation of the stannylene complex $(PR_3)_2Pd=SnR'_2$.⁸ Here, the reaction has a peculiar activation process with a stepwise motion of the phosphine ligands coordinated to the Pd atom as illustrated in Scheme 1.

The cleavage of the ethyne $C\equiv C$ π bond starts by the coordination of the $C\equiv C$ π bond to the Sn atom and is successfully attained by the rotation of the $(PR_3)_2Pd$ group around the Pd–Sn axis which promotes the orbital interactions between the Pd=Sn and ethyne. When the electronic configuration of the Pd=X bond is changed by the replacement of the Sn atom by the C atom, the activation has a completely different mechanism starting with the coordination of the ethyne not to the Sn atom but to the Pd atom.⁹

For the O–H bond activation, the reaction is not accompanied by the rotation of the $(PR_3)_2Pd$ group observed in the $C\equiv C$ π bond activation as presented by⁹



After the coordination of the H_2O oxygen to the Sn atom, the O–H bond is heterolytically broken and the hydrogen is transferred to the Pd atom as a proton. The activation mechanism is sensitively affected by the properties of the Pd=X bond as well; at the Pd=C bond, not the heterolytic cleavage but the homolytic cleavage takes place without the coordination of the

H_2O oxygen to the C atom, the reaction being rather heterolytic at the Pd=Si bond. A similar heterolytic cleavage was also found for the activation of the N–H bond of NH_3 with the lone pair electron.⁹

Now, as a matter of course, the following subjects on the σ and π bond activation at the Pd=Sn bond would arise based on our previously mentioned calculation results: (i) Is the activation of the C–H and H–H bonds without the lone pair electron other than the O–H and N–H bonds with the lone pair electron also heterolytic? (ii) Does the Pd fragment with the phosphine ligands rotate during the activation of the other π bonds of $C=C$ and $C=O$ with the lone pair electron? Are these reactions homolytic or heterolytic? (iii) What is the essential role of the Sn and P ligands in the heterolytic and homolytic activation? In concrete terms, how do these ligands control the reaction with or without rotation of the $(PR_3)_2Pd$ group? The problems for the activation mechanism which is closely correlated with the function of the ligand still remain unclear.

In the present study, to shed light on the issue with general interest for the type of σ and π bond cleavage, i.e., homolytic or heterolytic, that would be controlled by the ligand in the present case, the mechanism of the activation of the σ and π bonds at the Pd=X ($X = Sn, Si, C$) bonds was theoretically investigated using the density functional method (B3LYP) with the model complexes $(H_2PC_2H_4PH_2)Pd=XH_2$ having a chelate phosphine ligand. The typical simple molecules H_2O , CH_4 , and H_2 were adopted for the O–H, C–H, and H–H σ bond activation, respectively. For the π bond activation, the two kinds of double bonds, the $C=C$ of C_2H_4 and the $C=O$ of $HCHO$, were chosen in addition to the $C\equiv C$ of C_2H_2 . The activation at the Pd=X bonds was also compared with the independent activation at X of the free XH_2 and at Pd of the $(H_2PC_2H_4-PH_2)Pd$ fragment. Following the explanation of the calculation method in section 2, σ bond activation is discussed in the next three subsections: O–H bond activation in section 3.1, C–H bond activation in section 3.2, and H–H bond activation in section 3.3. The π bond activation of $C\equiv C$, $C=C$, and $C=O$ is discussed in section 3.4. The conclusions are listed in section 4.

2. Computational Details

All calculations were performed using the Gaussian98 program.¹⁰ The calculations of the energetics as well as the geometry optimizations were carried out at the B3LYP level of theory, which consists of a hybrid Becke + Hartree–Fock exchange and Lee–Yang–Parr correlation functional with nonlocal corrections.¹¹ The basis set used (hereinafter referred to as basis set I) is the 6-31G** level for the H, C, O, and Si atoms of water, methane, dihydrogen, ethyne, ethene, formaldehyde, stannylene, silylene, and carbene molecules, the 6-31G level for the C and H atoms, and the 6-31G* level for the P atom of

(7) (a) Krause, J.; Pluta, C.; Pörschke, K.-R.; Goddard, R. *J. Chem. Soc., Chem. Commun.* **1993**, 1254. (b) Krause, J.; Haack, K.-J.; Pörschke, K.-R.; Gabor, B.; Goddard, R.; Pluta, C.; Seevogel, K. *J. Am. Chem. Soc.* **1996**, *118*, 804.

(8) Sahnoun, R.; Matsubara, T.; Yamabe, T. *Organometallics* **2000**, *19*, 5661.

(9) Matsubara, T. *Organometallics* **2001**, *20*, 1462.

(10) Frisch, M. J.; Trucks, G. W.; Schlegel, H. B.; Scuseria, G. E.; Robb, M. A.; Cheeseman, J. R.; Zakrzewski, V. G.; Montgomery, J. A., Jr.; Stratmann, R. E.; Burant, J. C.; Dapprich, S.; Millam, J. M.; Daniels, A. D.; Kudin, K. N.; Strain, M. C.; Farkas, O.; Tomasi, J.; Barone, V.; Cossi, M.; Cammi, R.; Mennucci, B.; Pomelli, C.; Adamo, C.; Clifford, S.; Ochterski, J.; Petersson, G. A.; Ayala, P. Y.; Cui, Q.; Morokuma, K.; Malick, D. K.; Rabuck, A. D.; Raghavachari, K.; Foresman, J. B.; Cioslowski, J.; Ortiz, J. V.; Stefanov, B. B.; Liu, G.; Liashenko, A.; Piskorz, P.; Komaromi, I.; Gomperts, R.; Martin, R. L.; Fox, D. J.; Keith, T.; Al-Laham, M. A.; Peng, C. Y.; Nanayakkara, A.; Gonzalez, C.; Challacombe, M.; Gill, P. M. W.; Johnson, B.; Chen, W.; Wong, M. W.; Andres, J. L.; Gonzalez, C.; Head-Gordon, M.; Replogle, E. S.; Pople, J. A. *Gaussian 98*; Gaussian, Inc.: Pittsburgh, PA, 1998.

(11) (a) Lee, C.; Yang, W.; Parr, R. G. *Phys. Rev. B* **1988**, *37*, 785. (b) Becke, D. J. *Chem. Phys.* **1993**, *98*, 5648.

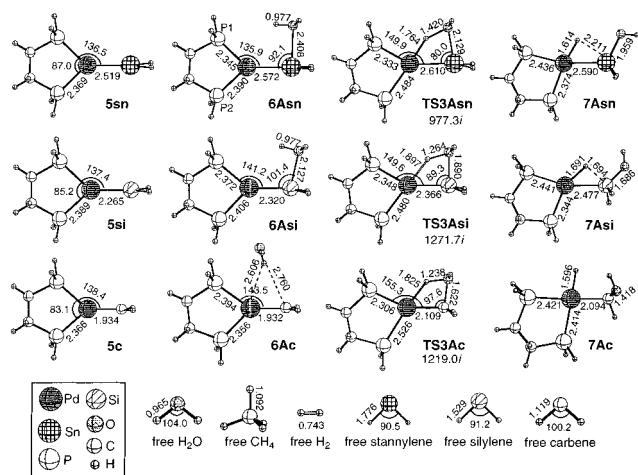


Figure 2. B3LYP/I-optimized structures (in Å and deg) of the reactants **5**, the intermediates **6A**, transition states **TS3A**, and the products **7A** for the activation of the water O–H bond at the Pd=X (X = Sn, Si, C) bonds of the $(\text{H}_2\text{PC}_2\text{H}_4\text{PH}_2)\text{Pd}=\text{XH}_2$ complexes **5** and the free molecules. The imaginary frequencies (cm^{-1}) for the transition states **TS3A** are presented together.

the spectator ligand $\text{H}_2\text{PC}_2\text{H}_4\text{PH}_2$. For Pd, the triple ζ (5s,6p,4d,1f)/[3s,3p,3d,1f] augmented by an additional single set of f orbitals with an exponent of 1.472¹² and the effective core potential (ECP) determined by Hay–Wadt¹³ to replace the core electrons except for the 18 electrons in the valence shell were used, and for Sn, the (3s,3p)/[2s,2p] basis functions with a 5d polarization function with an exponent of 0.183¹⁴ and the Hay–Wadt ECP¹⁵ to replace the core electrons except for the 4 valence electrons were used.

All equilibrium structures and transition states were optimized without any symmetry restrictions, and were identified by the number of imaginary frequencies calculated from the analytical Hessian matrix. The reaction coordinates were followed from the transition state to the reactant and the product by the intrinsic reaction coordinate (IRC) technique.¹⁶ The important structures on the reaction coordinates are arbitrarily selected to know the reaction processes and are displayed together with the potential energy surfaces of the reactions. The energies in the solvent were also calculated by the polarized-continuum-model (PCM) approximation¹⁷ for the B3LYP/I-optimized equilibrium and transition state structures in the reaction systems $(\text{H}_2\text{PC}_2\text{H}_4\text{PH}_2)\text{Pd}=\text{SnH}_2 + \text{H}_2\text{O}$ (Figure 3) and $\text{SnH}_2 + \text{H}_2\text{O}$ (Figure 4) at the PCM-B3LYP/I level using tetrahydrofuran (THF) with dielectric constant $\epsilon = 7.58$ and water with dielectric constant $\epsilon = 78.39$, which were experimentally used. The electronic structure of the stannylene **5sn**, silylene **5si**, and carbene **5c** complexes (Table 1) and the molecular orbital interaction were examined by NBO and molecular orbital analyses. For the atomic charge and the charge of the molecule in the text, the Mulliken charge is presented unless otherwise indicated.

For the activation at the Pd=X bonds, the calculated energies relative to the free molecules and the $(\text{H}_2\text{PC}_2\text{H}_4\text{PH}_2)\text{Pd}=\text{SnH}_2$ complex **5sn** are shown. In the other cases, the energies presented are relative to the free molecules and the $(\text{H}_2\text{PC}_2\text{H}_4\text{PH}_2)\text{Pd}$ fragment. The labels for the

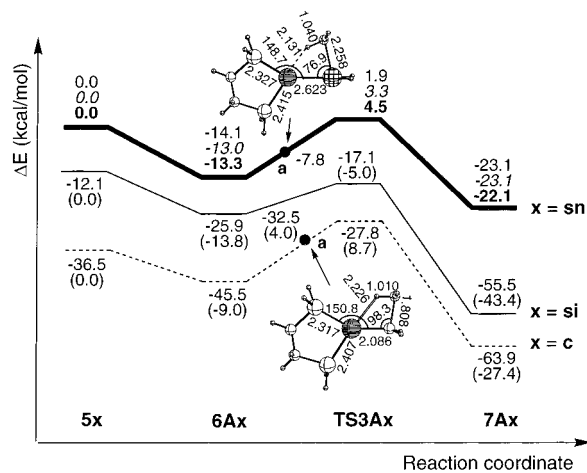


Figure 3. B3LYP/I potential energy surfaces (in kcal/mol) of the activation of the water O–H bond at the Pd=X (X = Sn, Si, C) bonds of the $(\text{H}_2\text{PC}_2\text{H}_4\text{PH}_2)\text{Pd}=\text{XH}_2$ complexes **5**. The boldface, normal, and dotted lines are for X = Sn, Si, C, respectively. The energies relative to **5sn** are presented (the numbers in the parentheses are the energies relative to the reactant **5x** in each reaction). For X = Sn, the energies in the solvent, THF ($\epsilon = 7.58$) and water ($\epsilon = 78.39$), at the PCM-B3LYP/I level are also given in italic type and boldface, respectively. The structures (in Å and deg) at points a on the reaction coordinates are displayed together.

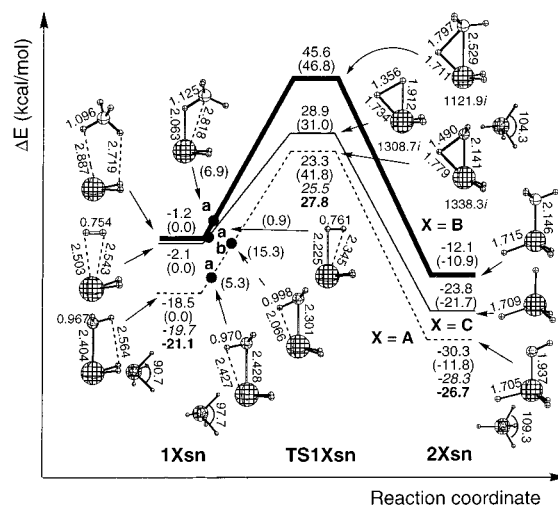


Figure 4. B3LYP/I potential energy surfaces (in kcal/mol) of the activation of the water O–H bond (dotted line), methane C–H bond (bold line), and the H_2 H–H bond (normal line) on the free stannylene, together with the optimized structures (in Å and deg) of the intermediates **1Xsn**, the transition states **TS1Xsn**, and the products **2Xsn** and the imaginary frequencies (cm^{-1}) for **TS1Xsn** at the B3LYP/I level. The energies relative to the free molecules are presented (the numbers in the parentheses are the energies relative to the reactant **1Xsn** in each reaction). For X = A, the energies in the solvent, THF ($\epsilon = 7.58$) and water ($\epsilon = 78.39$), at the PCM-B3LYP/I level are also given in italic type and boldface, respectively. The structures at points a and b on the reaction coordinates are displayed together. The top views are presented for some structures.

structures **A–G** for the substrates H_2O , CH_4 , H_2 , $\text{C}(\text{OH})\text{H}_3$, C_2H_4 , HCHO , and C_2H_2 , and **sn**, **si**, and **c** for the ligands, X = Sn, Si, C, are used, respectively.

3. Results and Discussion

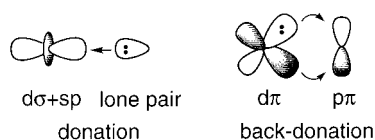
3.1. O–H Bond Activation. Although reported in a previous paper, the water O–H bond activation at the Pd=X (X = Sn, Si, C) bonds of the model complexes, $(\text{PH}_3)_2\text{Pd}=\text{XH}_2$, the reactants **5**, intermediates **6**, transition states **TS3**, and the products **7** were recalculated using the $(\text{H}_2\text{PC}_2\text{H}_4\text{PH}_2)\text{Pd}=\text{XH}_2$

- (12) Ehlers, A. W.; Böhme, M.; Dapprich, S.; Gobbi, A.; Höllwarth, A.; Jonas, V.; Köhler, K. F.; Stegmann, R.; Veldkamp, A.; Frenking, G. *Chem. Phys. Lett.* **1993**, *208*, 111.
- (13) Hay, P. J.; Wadt, W. R. *J. Chem. Phys.* **1985**, *82*, 299.
- (14) Huzinaga, S. *Physical Sciences Data 16, Gaussian Basis Sets for Molecular Calculations*; Elsevier: Amsterdam, 1984.
- (15) Wadt, W. R.; Hay, P. J. *J. Chem. Phys.* **1985**, *82*, 284.
- (16) Fukui, K.; Kato, S.; Fujimoto, H. *J. Am. Chem. Soc.* **1975**, *97*, 1.
- (17) (a) Cossi, M.; Barone, V.; Cammi, R.; Tomasi, J. *Chem. Phys. Lett.* **1996**, *255*, 327. (b) Fortunelli, A.; Tomasi, J. *Chem. Phys. Lett.* **1994**, *231*, 34. (c) Tomasi, J.; Persico, M. *Chem. Rev.* **1994**, *94*, 2027. (d) Floris, F.; Tomasi, J. *J. Comput. Chem.* **1989**, *10*, 616. (e) Pascual-Ahuir, J. L.; Silla, E.; Tomasi, J.; Bonaccorsi, R. *J. Comput. Chem.* **1987**, *8*, 778. (f) Mieritus, S.; Tomasi, J. *J. Chem. Phys.* **1982**, *65*, 239. (g) Mieritus, S.; Scrocco, E.; Tomasi, J. *J. Chem. Phys.* **1981**, *55*, 117.

Table 1. NBO Analysis of the $(\text{H}_2\text{PC}_2\text{H}_4\text{PH}_2)\text{Pd}=\text{XH}_2$ ($\text{X} = \text{Sn}, \text{Si}, \text{C}$) Complexes **5** at the B3LYP/I Level

	Pd–X bond				AO occupation		
	occup	% Pd	% s	% p	% d	Pd($d\pi$)	X($p\pi$)
5sn	σ : 1.91	18.2	97.7	0.3	2.0	1.77	0.34
	π : 1.97	89.3	0.0	0.0	100.0		
5si	σ : 1.94	18.0	97.3	0.3	2.4	1.73	0.41
	π : 1.98	77.5	0.0	0.2	99.8		

complexes having the chelate phosphine ligand and are presented in Figure 2. The electronic character of the Pd=X bonds, which significantly affects the activation mechanism, is determined by two kinds of orbital interactions by the charge transfer between the Pd and X atoms, i.e., the σ donation of the lone pair electron of the X atom to the hybridized $d\sigma + sp$ orbital of the Pd atom and the π back-donation from the occupied $d\pi$ orbital of the Pd atom to the unoccupied $p\pi$ orbital of the X atom:



The unoccupied $p\pi$ orbital of the X atom interacts with the occupied $d\pi$ orbital of the Pd atom enhanced by the small P–M–P bite angle of $83\text{--}87^\circ$ ¹⁸ so that the H–Sn–H plane is perpendicular to the P–M–P plane as shown in the reactants **5**. As shown in Table 1, the natural orbital population for the $d\pi$ orbital of the Pd atom decreased in the order $\text{Sn} > \text{Si} > \text{C}$, while it increased for the $p\pi$ orbital of the X atom in the opposite order, indicating that the π back-donation is stronger in the order $\text{C} > \text{Si} > \text{Sn}$.

This is reflected by the parameter $\angle\text{P–M–P}$ in **5** with the order $\text{Sn} > \text{Si} > \text{C}$ even with the chelate ligand. The NBO results presented in Table 1 also indicate that the Pd–X π bond is more polarized for $\text{X} = \text{Sn}$ than for $\text{X} = \text{C}$. However, in fact, for $\text{X} = \text{Si}$, the Pd $d\pi$ electron was a lone pair electron. The negative charge of the XH_2 counterpart was much larger for CH_2 (-0.147 e) than for SnH_2 (-0.054 e) and SiH_2 (-0.041 e), in accordance with the fact that the electronegativity increases with the order C (2.55) $>$ Sn (1.96) \geq Si (1.90).¹⁹

During activation of the water O–H bond at the Pd=X bond of the $(\text{H}_2\text{PC}_2\text{H}_4\text{PH}_2)\text{Pd}=\text{XH}_2$ complex to produce the product **7**, there is no significant change in the geometric feature and in the shape of the potential energy surface compared with the case of the $(\text{PH}_3)_2\text{Pd}=\text{XH}_2$ complexes.⁹ The strong electron donor oxygen of water first coordinates to the Sn with the O–Sn distance of 2.408 Å by the electron donation of the lone pair electron of the oxygen to the unoccupied p orbital of the Sn to produce the intermediate **6Asn**, as presented in Figure 2. The Pd–X–O angle is somewhat smaller because steric stress between the $(\text{H}_2\text{PC}_2\text{H}_4\text{PH}_2)\text{Pd}$ and $\text{X}(\text{H}_2\text{O})\text{H}_2$ moieties is reduced due to the small bite angle of the $\text{H}_2\text{PC}_2\text{H}_4\text{PH}_2$ chelate ligand compared with the case of the $(\text{PH}_3)_2\text{Pd}=\text{XH}_2$ complexes. The donation of the lone pair electron of the H_2O oxygen to the unoccupied p orbital of Sn depresses the electron donation

from the Pd $d\pi$ orbital to the unoccupied Sn p orbital to localize the electron on the Pd $d\pi$ orbital. Thereby, the Pd–Sn bond in **6Asn** is stretched by 0.053 Å compared with that in **5sn**. The Pd–P2 distance is also affected by the coordinated H_2O through the $d\pi\text{--}p\pi$ orbital and is longer by 0.045 Å than the Pd–P1 distance. The positive charge of the H_2O hydrogen is increased up to +0.349 e (+0.306 e in the free H_2O) in **6Asn**. In the transition state **TS3Asn**, the O–Sn bond is nearly formed and the nucleophile Pd extracts the positively charged H_2O hydrogen as a proton. The process of heterolytic cleavage of the O–H bond is well reflected by the molecular motion along the reaction coordinate from the intermediates **6Asn** to the transition state **TS3Asn** through point a (Figure 3), which is not synchronous; the coordination of the hydroxyl group of water as OH^- and the enhancement of the nucleophilicity of the Pd is the first process, and in the second process, the proton migrates from the H_2O oxygen to the Pd atom, where Pd(0) is oxidized to Pd(II). The O–Sn distance is already reduced to 2.258 Å at point a although the O–H bond distance of the water is only stretched 6.4% compared with that in **6Asn**. On the other hand, the Pd–Sn distance is elongated to 2.623 Å to become a single bond. As shown by the large P–Pd–Sn angle of 148.7° , the $\text{H}_2\text{PC}_2\text{H}_4\text{PH}_2$ ligand rotates counterclockwise around the Pd atom on the P–Pd–P plane keeping the bite angle of 87° in order to locate one of the electron donative phosphines trans to the proton. The O–Sn–Pd angle is reduced to 76.9° , and the water hydrogen approaches the Pd. The positive charge of the water hydrogen is increased to +0.384 e, and the amount 0.245 e was calculated to be transferred from the $\text{Sn}(\text{H}_2\text{O})\text{H}_2$ counterpart to the $d\pi$ orbital of the Pd along the H–O–Sn–Pd linkage.

In the product **7Asn**, the hydrido ligand tends to bridge over the Pd–Sn bond, and, thereby, the Pd–P2 distance is shorter by 0.062 Å than the Pd–P1 distance because the electron donation from the P2 to the Pd is promoted due to the delocalization of the electron on the hydrido into the Pd–H–Sn region.

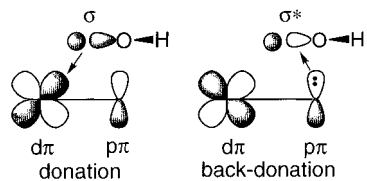
Even if the Sn atom is replaced by the Si atom, the same mechanism of the heterolytic cleavage of the water O–H bond is not changed. The structural features of the intermediate **6Asi**, transition state **TS3Asi**, and the product **7Asi** are similar to the case of $\text{X} = \text{Sn}$, although **TS3Asi** is more reactant-like. In **6Asi**, however, the p orbital of Si slightly inclines with the somewhat larger O–Sn–Pd angle of 101.4° , avoiding the π back-donation from the occupied $d\pi$ orbital of the Pd to interact more strongly with the orbital of the lone pair electron of the H_2O oxygen.

In the case of $\text{X} = \text{C}$, the water O–H bond activation becomes homolytic. The more localized π electron on the $p\pi$ orbital of the C (see above) does not allow the H_2O oxygen to coordinate to the C atom by the donation of the lone pair electron to the p orbital of the C atom in **6Ac**. Therefore, the H_2O hydrogen, which has a positive charge, bridges the electron-rich Pd=C by a weak electrostatic interaction. Here, it is worth noting that the Pd–P2 distance is shortened because the electron donation of the P2 to the Pd is enhanced to provide the electron for this electrostatic interaction through the P2–Pd–H(H_2O) linkage. Without the coordination of the H_2O oxygen to the C atom, the O–H bond bridges the Pd=C bond in the transition state **TS3Ac**. As shown by the structure at point a, the electron back-donation from the p orbital of the C to the O–H σ^* orbital

(18) Saillard, J.-Y.; Hoffmann, R. *J. Am. Chem. Soc.* **1984**, *106*, 2006.

(19) Pauling's values are presented. For example, see: *The Elements*, 2nd ed.; Emsley, J., Ed.; Oxford University Press: New York, 1991.

and then the donation from the O–H σ orbital to the $d\pi$ orbital of the Pd takes place to break the O–H bond as illustrated by



The hydrido H does not interact with the C atom in the product **7Ac**, which is different from the case of X = Sn, Si. The reaction path found for CH₄ (section 3.2) and H₂ (section 3.3), where the H₂O oxygen coordinates to the Pd first, did not exist.

As presented in Figure 3, the water O–H bond activation was exothermic for any Pd=X (X = Sn, Si, C) bonds of $(\text{H}_2\text{PC}_2\text{H}_4\text{PH}_2)\text{Pd}=\text{XH}_2$. All the intermediates, transition states, and products are slightly more stable when compared with $(\text{PH}_3)_2\text{Pd}=\text{XH}_2$,⁹ although the features of the potential energy surfaces are almost the same. The first process of the O–H bond breaking at the Pd=Sn bond, the O–Sn bond formation, requires the energy of 6.3 kcal/mol, which corresponds to about half the energy barrier of 16.0 kcal/mol. In the case of X = Si, the transition state **TS3Asi** is lower in energy than the reactant **5si** in contrast to the cases of X = Sn, C, and the energy barrier is reduced to 8.8 kcal/mol due to the large exothermicity of the reaction (43.4 kcal/mol). The energy barrier of 17.7 kcal/mol for X = C is the largest among X = Sn, Si, C, because the transition state **TS3Ac** is less stable than reactant **5c** by 8.7 kcal/mol, which would originate from the homolytic mechanism. The large amount of energy, i.e., 73% of the energy barrier, has to be spent for the approach of the water O–H bond to the Pd=C bond, which is ascribed to the strong repulsion between the lone pair electron of the water oxygen and the localized electron on the p orbital of the C atom.

It has been experimentally reported that the free stannylene itself indicates the activation activity for the water O–H bond as mentioned in the Introduction. By combination with the Sn–H bond activation of the Sn(OH)H₃ at the Pd of the $(\text{H}_2\text{PC}_2\text{H}_4\text{PH}_2)\text{Pd}$, another path ii to produce **7Asn** presented in Figure 1 can be constructed. To compare the energetic preference with path i, path ii was also examined.

The H₂O similarly coordinates to the SnH₂ by the donation of the lone pair electron to the unoccupied p orbital of the SnH₂. The series of snapshots of the structures from **1Asn** to **TS1Asn** on the reaction coordinate indicates the stepwise structural change climbs the energy mountain as presented in Figure 4. The coordinated H₂O pivots to direct one of the hydrogens toward the lone pair electron on the Sn breaking the electrostatic interaction between the positively charged H₂O hydrogen and the negatively charged SnH₂ hydrogen (point a). The O–Sn distance is shortened to 2.301 Å, and the lone pair electron of the H₂O oxygen is directed toward the negatively charged SnH₂ hydrogens at point b. Thereby, the two hydrogens attached to the Sn move away from the H₂O by the repulsive interaction between them. The orbital of the lone pair electron of the SnH₂ moves up to attract the positively charged H₂O hydrogen so that the Sn–H(H₂O) distance is shortened to 2.066 Å. In the transition state **TS1Asn**, the OH[−] coordination and the proton migration to the lone pair electron of the SnH₂ is almost completed as shown by the short Sn–H (1.779 Å) and Sn–O

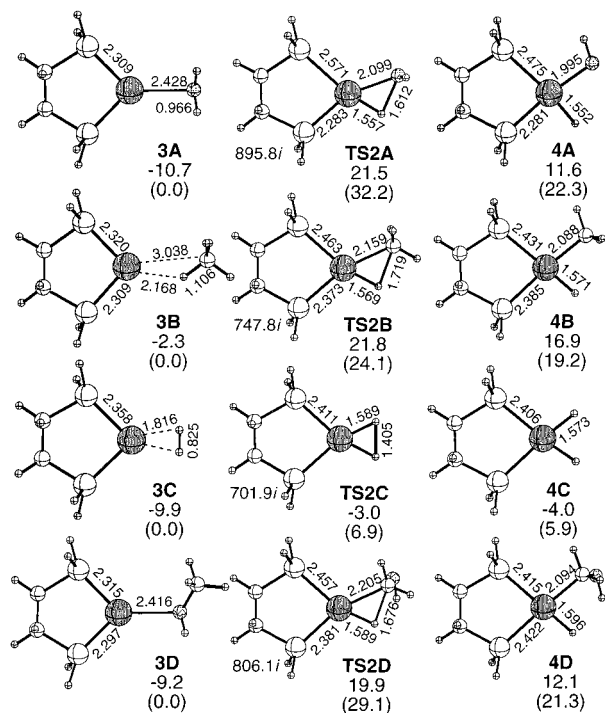


Figure 5. B3LYP/I-optimized structures (in Å and deg) of the intermediates **3**, the transition states **TS2**, and the products **4** for the activation of the water O–H bond, the methane C–H bond, the H–H bond of the H₂ molecule, and the C–H bond of C(OH)H₃ at the Pd of the $(\text{H}_2\text{PC}_2\text{H}_4\text{PH}_2)\text{Pd}$ fragment. Their energies relative to the free molecules and the imaginary frequencies (cm^{-1}) for the transition states **TS2** at the B3LYP/I level are also presented together. The values in parentheses are the energies relative to **3** in each reaction.

(2.141 Å) and the long O–H (1.490 Å) distances. Since the positive charge of the H₂O hydrogen is already increased to the maximum (+0.348 e) at point a, the energy of 10 kcal/mol from point a to point b would be required for the structural rearrangement mentioned above. The structure of the transition state **TS1Asn** largely deformed from the sp³-hybridized tetrahedron is considered to be the main reason for the large energy barrier of 41.8 kcal/mol.

The second step of path ii in Figure 1, the Sn–H oxidative addition of the Sn(OH)H₃ to the $(\text{H}_2\text{PC}_2\text{H}_4\text{PH}_2)\text{Pd}$ fragment to form **7Asn**, was downhill without the energy barrier, which indicates that the first step of the O–H activation by the free SnH₂ is rate-determining. Judging from the energy barrier, it is obvious that path i is much more facile than path ii, which is consistent with the experimental result.⁴ This calculation result did not change even if the solvent effect is taken into account. As shown in Figures 3 and 4, both the THF solvent and water experimentally used did not significantly affect the potential energy surfaces.

The energy barrier for the well-known activation in the homolytic manner at the Pd of the $(\text{H}_2\text{PC}_2\text{H}_4\text{PH}_2)\text{Pd}$ fragment was calculated to be 32.2 kcal/mol for the water O–H bond as presented in Figure 5, which is 2 times larger than that for the heterolytic activation at the Pd=Sn bond. Although in the starting complex **3A** the H₂O oxygen coordinates to the Pd by the donation of its lone pair electron to the Pd, the oxygen coordination is first broken and the O–H activation homolytically occurs in the P–Pd–P plane by electron donation from the O–H σ orbital to the Pd $d\sigma + sp$ orbital and the π back-donation from the Pd $d\pi$ orbital to the O–H σ^* orbital in the

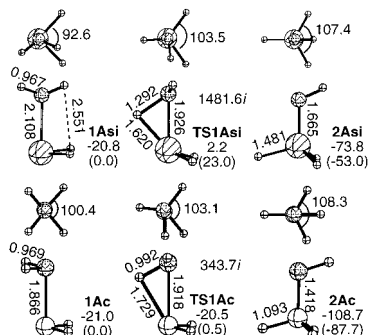


Figure 6. B3LYP/I-optimized structures (in Å and deg) of the intermediates **1A**, the transition states **TS1A**, and the products **2A** for the activation of the water O–H bond on the free silylene and carbene, together with their energies relative to the free molecules and the imaginary frequencies (cm^{-1}) for the transition states **TS1A** at the B3LYP/I level. The values in the parentheses are the energies relative to **1A** in each reaction.

transition state **TS2A**, where the lone pair electron on the oxygen is out of the P–Pd–P plane. It should be noted that the charge of the H_2O is negative (-0.321 e) in **TS2A** due to the strong electron back-donation from the Pd. Even though the energy is compared with that of the free H_2O and the $(\text{H}_2\text{PC}_2\text{H}_4\text{PH}_2)\text{Pd}$ fragment, the transition state **TS2A** is higher by 21.5 kcal/mol. Thus, the heterolytic O–H bond activation at the Pd=Sn bond requires the least energy of only 16.0 kcal/mol because of the bifunction of the Pd and Sn atoms mentioned above.

The energy barrier for the water O–H bond activation at the X of the free XH_2 was reduced to 23.0 kcal/mol for $X = \text{Si}$ and to 0.5 kcal/mol in the case of $X = \text{C}$, since the exothermicity largely increases (Figure 6). On the other hand, the oxidative addition of the C–H bond of the $\text{C}(\text{OH})\text{H}_3$ **2Ac** to the $(\text{H}_2\text{PC}_2\text{H}_4\text{PH}_2)\text{Pd}$ fragment requires the large energy barrier of 29.1 kcal/mol (Figure 5), although that of the Si–H bond of the $\text{Si}(\text{OH})\text{H}_3$ **2Asi** as well as that of the Sn–H bond of the $\text{Sn}(\text{OH})\text{H}_3$ **2Asn** is downhill.²⁰ That is, this indicates that the rate-determining step of path ii is switched from the first step to the second step in the case of $X = \text{C}$. However, in all the cases of $X = \text{Sn}, \text{Si}, \text{C}$, path i is more facile than path ii.

3.2. C–H Bond Activation. The activation of the other σ bond without the lone pair electron, the C–H of CH_4 and the H–H of H_2 , is discussed in this and the next sections. The CH_4 molecule without the lone pair electron does not coordinate to the Sn in **6Bsn** as shown by the long Sn–H distance of 3.603 Å (Figure 7). Starting from **6Bsn**, the C–H bond of the CH_4 molecule first approaches the Sn in the η^2 fashion at point a on the potential energy surface (Figure 8).

Although the structural feature is similar to the case of H_2O (see the structure at point a on the potential energy surface displayed in Figure 3), the distance of C–Sn (2.793 Å) is very long. The CH_4 interferes with the electron π back-donation from the Pd $d\pi$ to the Sn p orbital breaking into the interaction between these orbitals, which localizes the electron on the Pd $d\pi$ orbital to enhance the nucleophilicity of the Pd. Therefore, the P–Pd–Sn angle is already enlarged to 142.1° , and the Pd–Sn distance is lengthened to 2.623 Å, indicating the single bond. As shown by the short H–Sn distance of 2.108 Å, the electron of the C–H bond is incipiently delocalized in the Sn–

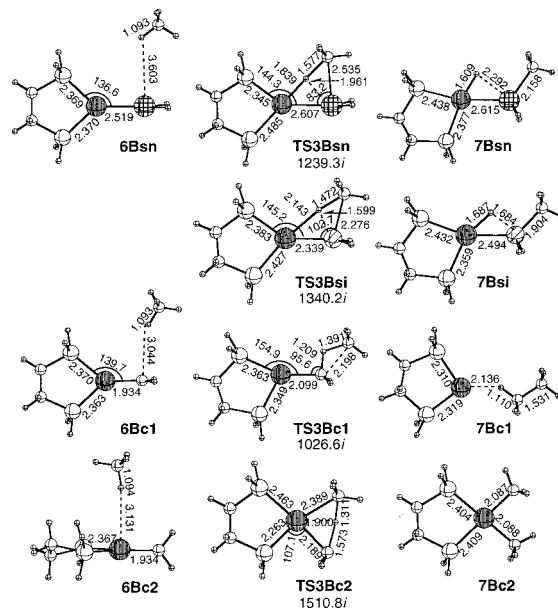


Figure 7. B3LYP/I-optimized structures (in Å and deg) of the intermediates **6B**, the transition states **TS3B**, and the products **7B** for the activation of the methane C–H bond at the Pd=X ($X = \text{Sn}, \text{Si}, \text{C}$) bonds of the $(\text{H}_2\text{PC}_2\text{H}_4\text{PH}_2)\text{Pd}=\text{XH}_2$ complexes **5**. The imaginary frequencies (cm^{-1}) for the transition states **TS3B** are presented together.

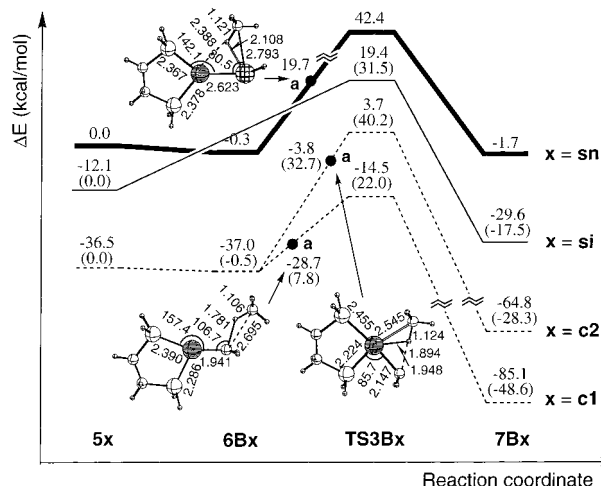


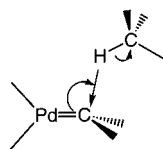
Figure 8. B3LYP/I potential energy surfaces (in kcal/mol) of the activation of the methane C–H bond at the Pd=X ($X = \text{Sn}, \text{Si}, \text{C}$) bonds of the $(\text{H}_2\text{PC}_2\text{H}_4\text{PH}_2)\text{Pd}=\text{XH}_2$ complexes **5**. The boldface, normal, and dotted lines are for $X = \text{Sn}, \text{Si}, \text{C}$, respectively. The energies relative to **5sn** are presented (the numbers in parentheses are the energies relative to the reactant **5x** in each reaction). The structures (in Å and deg) at points a on the reaction coordinates are displayed together.

H–C part. On the way from point a to the transition state **TS3Bsn**, the C–H, whose axis is directed toward the nucleophile Pd, is elongated and the electron for the Sn–H–C bridge is left for the C–Sn bonding. The C–H hydrogen, thus, bridges the C–Sn bond as a proton and is finally extracted by the occupied $d\pi$ orbital of the Pd. In the product **7Bsn**, the hydrido ligand tends to bridge the Pd–Sn bond, which is similar to the case of H_2O .

The reactant, which corresponds to **6Bsn** for $X = \text{Sn}$, was not found as an equilibrium structure in the case of $X = \text{Si}$. In the transition state **TS3Bsi**, the CH_4 hydrogen as a proton is more strongly attracted by the electronegative Si atom so that the Si–C axis inclines away from the Pd.

(20) It has been theoretically indicated so far that the Si–H bond activation is much easier than the C–H bond activation; for example, see: Koga, N.; Morokuma, K. *J. Am. Chem. Soc.* **1993**, *115*, 6883.

In the case of $\text{X} = \text{C}$, the CH_4 hydrogen has an electrostatic interaction with the localized π electron on the p orbital of the C atom in **6Bc1**. Starting from **6Bc1**, the CH_4 hydrogen migrates as a proton not to the Pd atom but to the C atom passing through point a, where the P–Pd–C angle becomes large to enhance the localization of the π electron on the p orbital of the C atom. The positive charge of the CH_4 hydrogen increases to +0.195 e (+0.115 e in the free CH_4) at point a and up to +0.224 e in the transition state **TS3Bc1**. It should be noted here that the CH_4 hydrogen belongs to the carbene carbon rather than to the methane carbon in **TS3Bc1** and the other reaction, the $\text{S}_{\text{N}}2$ nucleophilic substitution, is already started; the nucleophile CH_4 carbon, which is mostly negatively charged by the bond alternation illustrated below, attacks the carbene carbon. The



positive charge of the $(\text{H}_2\text{PC}_2\text{H}_4\text{PH}_2)\text{Pd}$ fragment (+0.134 e) at point a becomes negative (−0.045 e) in **TS3Bc1**, indicating the electron flow from the CH_4 carbon to the Pd via carbene carbon during the initial stage of the $\text{S}_{\text{N}}2$ substitution reaction. The Pd–C bond distance of 2.099 Å in **TS3Bc1** is already slightly longer than that in **7Ac**, which is a single bond. After passing through the transition state **TS3Bc1**, the tetrahedron configuration of the carbene carbon is inverted with the approach of the methane carbon and the Pd–C bond is broken to form the product **7Bc1**. Here, the oxidation number of the Pd changes from II to 0 because the lone pair electron of the carbene is left on the Pd. Thus, the CH_4 hydrogen is extracted not by the Pd atom but by the C atom which is the nucleophile.

Since the Pd $d\pi$ orbital is electron deficient in the case of $\text{X} = \text{C}$, as one would expect, another path for the activation of the methane C–H bond, where methane first approaches not the carbene carbon but the Pd atom, was found. As presented in Figure 7, the incoming CH_4 weakly coordinates to the Pd in the reactant **6Bc2**, and slides into the P–Pd–P plane at the transition state **TS3Bc2** to transfer the hydrogen as a proton to the carbene carbon with the lone pair electron on the p orbital received from the Pd $d\pi$ orbital. The positive charge of the CH_4 hydrogen is enhanced to +0.247 e during the first stage of the CH_4 migration into the P–Pd–P plane without the C–H bond breaking (point a in Figure 8). The C–H σ electron is localized on the negatively charged CH_4 carbon and is donated to the unoccupied Pd $d\pi$ orbital. Both the C–Pd bond formation and the proton transfer to the carbene carbon synchronously take place during the second stage. It would be interesting that a similar reaction path was not found for the water O–H bond activation.

The potential energy surfaces of the methane C–H bond activation at the Pd= X bonds are presented together in Figure 8. The reaction is energetically almost neutral for $\text{X} = \text{Sn}$ and requires the large energy barrier of 42.5 kcal/mol. Although the reaction becomes 17.5 kcal/mol exothermic when the atom X is Si, the energy barrier is still large (31.5 kcal/mol). The energy barrier for the reaction with $\text{X} = \text{C}$ where ethane is finally produced was reduced to 22.5 kcal/mol. However, another reaction with $\text{X} = \text{C}$ needs the large energy barrier of

40.7 kcal/mol, most of the energy being used for the deformation of the $(\text{H}_2\text{PC}_2\text{H}_4\text{PH}_2)\text{Pd}=\text{CH}_2$ structure (see the structure and the energy at point a).

The methane C–H bond activation on the free SnH_2 also has the heterolytic mechanism (Figure 4). The methane weakly interacts with the stannylene by both electron donation from the C–H σ orbital to the unoccupied p orbital of the Sn and the electrostatic interaction of the positively charged methane hydrogen with one of the negatively charged stannylene hydrogens in the reactant **1Bsn**. At point a on the reaction coordinate, the methane hydrogen is located just above the p orbital of Sn, and the electron of 0.107 e flows from the methane C–H bond to the p orbital of the Sn to make the Sn–H(methane) interaction stronger, which results in the bridge of the methane hydrogen over the Sn–C. However, in the transition state **TS1Bsn**, the methane is only slightly negatively charged (−0.084 e), because the methane hydrogen migrates as a proton toward the lone pair electron of the stannylene, leaving the electron for the C–Sn bonding. The Sn of the product **2Bsn** has a tetrahedral structure by the sp^3 orbital rearrangement, which is similar to the case of the water O–H bond activation. The energy barrier of 46.8 kcal/mol is as large as 42.7 kcal/mol calculated for the activation at the Pd= Sn bond, which indicates that the combination of the Pd= Sn does not effectively function for the methane C–H activation. This sharply contrasts with the case of H_2O . On the other hand, the classical homolytic cleavage of the methane C–H bond at the Pd of the $(\text{H}_2\text{PC}_2\text{H}_4\text{PH}_2)\text{Pd}$ fragment requires only half the energy barrier (24.1 kcal/mol) as presented in Figure 5. Upon comparison between the water O–H and the methane C–H bond activation, it is quite interesting that the energy barrier is larger for the water O–H bond than for the methane C–H bond in the homolytic cleavage on the independent $(\text{H}_2\text{PC}_2\text{H}_4\text{PH}_2)\text{Pd}$ fragment, while it is much smaller for the water O–H bond than for the methane C–H bond in the heterolytic cleavage at the Pd= Sn bond. Thus, the water O–H and the methane C–H bonds prefer the heterolytic activation at the Pd= Sn bond and the homolytic activation on the $(\text{H}_2\text{PC}_2\text{H}_4\text{PH}_2)\text{Pd}$ fragment, respectively.²¹

3.3. H–H Bond Activation. The activation of the H–H σ bond of the H_2 molecule has a mechanism similar to the case of the C–H σ bond of CH_4 . For $\text{X} = \text{Sn}$, the H_2 molecule weakly coordinates to the Sn atom by the side-on mode via the electron donation from the H_2 σ orbital to the unoccupied Sn p orbital in the reactant **6Csn** as presented in Figure 9.

The coordinated H_2 molecule approaches the Sn atom by keeping η^2 coordination, which localizes the electron contributing the π back-donation from the Pd $d\pi$ orbital to the Sn p orbital on the Pd $d\pi$ orbital. It was found that the amount of 0.095 e is transferred from the H_2 -coordinated SnH_2 to the Pd $d\pi$ orbital through the orbital interaction between the Pd $d\pi$ and the Sn p orbitals. The H_2 inclines toward the Pd $d\pi$ orbital without rotation of the $(\text{H}_2\text{PC}_2\text{H}_4\text{PH}_2)\text{Pd}$ group (see section 3.4 for the rotation), breaking into the orbital interaction between the Pd $d\pi$ and the Sn p, the Pd–Sn bond is stretched to 2.676 Å, and the P–Pd–Sn angle is increased to 145.8° at point a on the reaction coordinate (see Figure 10). Passing through the

(21) It is worth noting that the energy barrier for the activation of the water O–H bond at the Pd= Sn bond (16.0 kcal/mol) is smaller than that for the activation of the methane C–H bond at the Pd of the free $(\text{H}_2\text{PC}_2\text{H}_4\text{PH}_2)\text{Pd}$ fragment (24.1 kcal/mol), although the bond energy of the water O–H (118 kcal/mol) is larger than that of the methane C–H (103 kcal/mol).

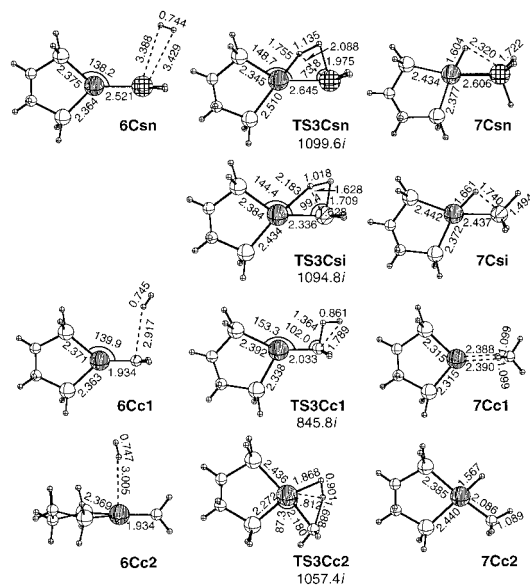


Figure 9. B3LYP/I-optimized structures (in Å and deg) of the intermediates **6C**, the transition states **TS3C**, and the products **7C** for the H–H bond activation of the H₂ molecule at the Pd=X (X = Sn, Si, C) bonds of the (H₂PC₂H₄PH₂)Pd=XH₂ complexes **5**. The imaginary frequencies (cm⁻¹) for the transition states **TS3C** are presented together.

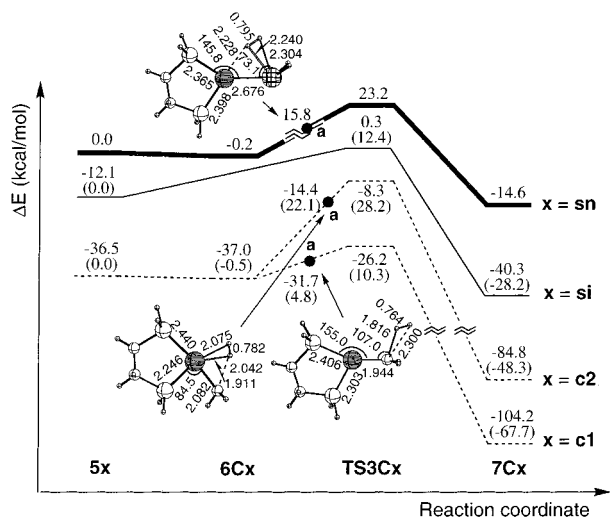


Figure 10. B3LYP/I potential energy surfaces (in kcal/mol) of the H–H bond activation of the H₂ molecule at the Pd=X (X = Sn, Si, C) bonds of the (H₂PC₂H₄PH₂)Pd=XH₂ complexes **5**. The energies relative to **5sn** are presented (the numbers in parentheses are the energies relative to the reactant **5x** in each reaction). The structures (in Å and deg) at points a on the reaction coordinates are displayed together.

transition state **TS3Csn**, where the H on the Pd side is positively charged (+0.043 e) and another H is negatively charged (−0.086 e), the heterolytic cleavage of the H–H bond takes place to form the product **7Csn**; the H⁺ is extracted by the nucleophile Pd and the H[−] is left on the Sn electrophile.

Even though the X atom is Si, the activation of the H–H bond proceeds by the same heterolytic mechanism. However, the reactant with the H₂ coordinated to the Si atom was not found as an equilibrium structure, due to the extremely weak interaction of the H₂ molecule with the Si atom. Since the electron on the p orbital of the Si is transferred back to the Pd d π orbital in the transition state **TS3Csi** by the approach of the

H₂ molecule to the Si via the electron donation from the H–H σ orbital to the Si p orbital, the character of the Si atom, which strongly binds the H atom, is obviously reflected by the short Si–H distances of 1.628 and 1.709 Å, despite the early transition state with the short H–H (1.018 Å) and the long Pd–H (2.183 Å) distances.

In the case of X = C, there exist two paths for the heterolytic activation of the H–H bond, which is similar to the case of CH₄; one produces the methane-coordinated complex **7Cc1** via the transition state **TS3Cc1** starting from **6Cc1** and another produces the methyl–hydrido complex **7Cc2** via the transition state **TS3Cc2** starting from **6Cc2** (Figure 9). The H₂ molecule first approaches by the end-on mode to the C atom in the former and to the Pd atom in the latter. In both paths, the enlargement of the P–Pd–C angle, which promotes the localization of the π electron on the C p orbital, induces the reaction (see the structures at points a on the reaction coordinates in Figure 10). In the transition state **TS3Cc1**, the H–H bond is only 16% stretched although the H–C distance of 1.364 Å is short. The H, which is extracted as a proton by the C atom, has the positive charge of +0.141 e. Another H, which is negatively charged, attacks the carbene carbon as an H[−] to start the S_N2 substitution at the carbene carbon as shown by the already short C–H distance of 1.789 Å. The heterolytic cleavage of the H–H bond and the S_N2 substitution, in fact, simultaneously proceed to form methane. On the other hand, in the transition state **TS3Cc2**, the H₂ molecule slides into the P–Pd–C plane. The H extracted as a proton by the C atom has the positive charge of +0.156 e, and the electron in the H–H σ orbital is localized on another H atom which coordinates to the Pd as an H[−] by the electron donation to the unoccupied Pd d orbital.

Compared with the case of CH₄, as presented in Figure 10, the energy barrier for the heterolytic cleavage of the H–H bond at the Pd=X bonds are much smaller for each case of X = Sn, Si, C due to the large exothermicity of the reaction, the trend in energy barrier, C > Sn > Si, being the same.

In the well-known homolytic cleavage of the H–H bond at the Pd of the (H₂PC₂H₄PH₂)Pd fragment, a further smaller energy of only 6.9 kcal/mol is needed (see Figure 5). In contrast, the heterolytic activation of the H–H bond at the Sn of the free SnH₂ to form SnH₄, where the H[−] coordinates to the unoccupied Sn p orbital and the H⁺ migrates to the lone pair electron of the SnH₂, requires the large energy barrier of 31.0 kcal/mol (see Figure 4).

3.4. C≡C, C=C, and C=O Bond Activation. We have reported in a previous paper that the first process of the catalytic cycle of the stannole formation is the activation of the C₂H₂ π bond at the Pd=Sn bond of (PH₃)₂Pd=SnH₂ to produce the 1,2-palladastannete complex.⁸ The reason this reaction smoothly proceeds was ascribed to the peculiar behavior of the phosphine ligand as mentioned in the Introduction. In this section, the activation of the π bond of ethyne, ethene, and formaldehyde at the Pd=Sn bond is discussed.

As shown by the activation of the ethyne C≡C π bond at the Pd=Sn bond of the (PH₃)₂Pd=SnH₂ complex (see Scheme 1), after the coordination of the ethyne C≡C π bond to the Sn atom in the η^2 fashion (**8Gsn'**), the (PH₃)₂Pd group rotates around the Pd–Sn axis by 90° (**10Gsn'**). Here, the η^2 interaction of the C≡C π bond with the Sn by the electron donation from the C≡C π orbital to the p orbital of the Sn is strengthened,

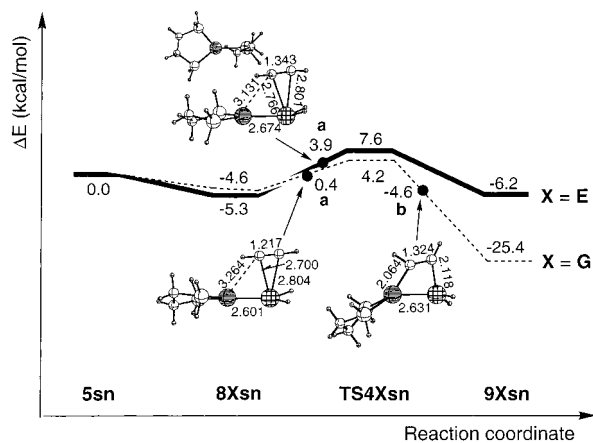
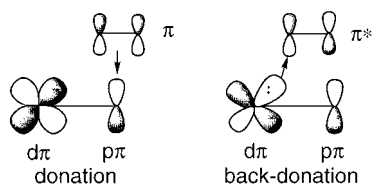


Figure 11. B3LYP/I potential energy surfaces (in kcal/mol) of the activation of the ethyne C≡C (dotted line)⁹ and the ethene C=C (bold line) π bonds at the Pd=Sn bond of the $(\text{H}_2\text{PC}_2\text{H}_4\text{PH}_2)\text{Pd}=\text{SnH}_2$ complex **5sn**. The structures (in Å and deg) at points a and b on the reaction coordinates are displayed together.

because the π back-donation from the $d\pi$ orbital of the Pd atom to the p orbital of the Sn atom is remarkably reduced by this rotation. In addition, the electron donation from the Pd $d\pi$ orbital to the ethyne C≡C π^* orbital is enhanced in the transition state (**TS4Gsn'**) as presented below. After passing through the transition state, the $(\text{PH}_3)_2\text{Pd}$ rotates back to form the 1,2-palladastannete complex (**9Gsn'**). Thus, the merit of the rotation of the $(\text{PH}_3)_2\text{Pd}$ group is that both the electron donation in **10Gsn'** and back-donation in **TS4Gsn'** to break the C≡C π bond are strengthened.



When the chelate ligand, $\text{H}_2\text{PC}_2\text{H}_4\text{PH}_2$, is used instead of the $(\text{PH}_3)_2$, the structure **10Gsn'** as an equilibrium structure disappears. However, it was found that the reaction undergoes a similar structure at point a on the reaction coordinate between **8Gsn** and **TS4Gsn** as presented in Figure 11. The energy required for the structural rearrangement from **8Gsn** to the structure at point a was only 5.7 kcal/mol. After passing through the transition state **TS4Gsn**, the Pd–C and Sn–C bonds are first formed at point b and then the $(\text{H}_2\text{PC}_2\text{H}_4\text{PH}_2)\text{Pd}$ group rotates back.²²

The activation of the ethene C=C π bond also follows the same stepwise reaction with the rotation of the $(\text{H}_2\text{PC}_2\text{H}_4\text{PH}_2)\text{Pd}$ group. The ethene C=C π bond coordinates to the Sn atom by the η^2 mode in **8Esn** as presented in Figure 12 by the donation of the π electron to the p orbital of the Sn. This coordination is much weaker than the coordination of the H_2O oxygen, and the ethene inclines away from the Pd. Since the π back-donation from the Pd $d\pi$ orbital to the Sn p orbital is weakened by this coordination, the Pd–Sn bond is stretched by 0.04 Å and the rotation of the $(\text{H}_2\text{PC}_2\text{H}_4\text{PH}_2)\text{Pd}$ group around

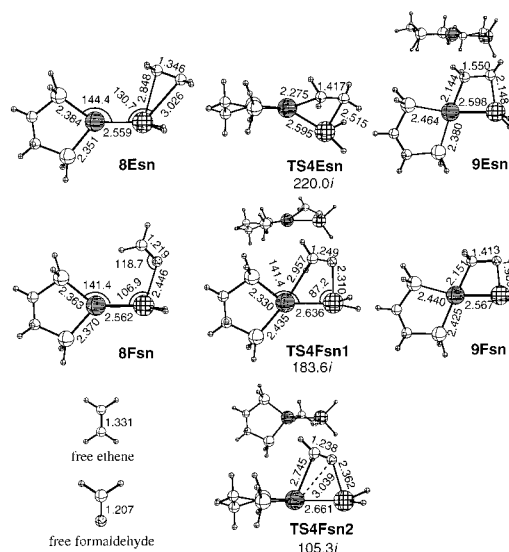


Figure 12. B3LYP/I-optimized structures (in Å and deg) of the intermediates **8**, the transition states **TS4**, and the products **9** for the activation of the ethene C=C and the formaldehyde C=O π bonds at the Pd=Sn bond of the $(\text{H}_2\text{PC}_2\text{H}_4\text{PH}_2)\text{Pd}=\text{SnH}_2$ complex **5sn** and the free molecules. The imaginary frequencies (cm^{-1}) for the transition states **TS4** are presented together. The top view is also displayed for **9Esn**, **TS4Fsn1**, and **TS4Fsn2**.

the Pd–Sn axis becomes easier. The rotation of the $(\text{H}_2\text{PC}_2\text{H}_4\text{PH}_2)\text{Pd}$ group by 90° strengthens the coordination of the ethene to the Sn as shown by the Sn–C(ethene) distances at point a on the reaction coordinate (Figure 11), which is shorter than those in **8Esn**. On the other hand, the Pd–Sn bond is further weakened, indicating a single bond (2.674 Å). The structure at point a does not exist as an equilibrium structure, which is similar to the case of ethyne. The orientation of the coordinated ethene somewhat deviates from the Pd–Sn axis, avoiding the repulsion between the hydrogens of the ethene and the SnH_2 . The electron back-donation from the $d\pi$ orbital perpendicular to the P–Pd–P plane to the ethene π^* orbital occurs at point a to break the ethene π bond (see the orbital picture presented above). In the transition state **TS4Esn**, the further rotation of the $(\text{H}_2\text{PC}_2\text{H}_4\text{PH}_2)\text{Pd}$ group around the Pd–Sn axis to form **9Esn** already significantly proceeds due to the late transition state. One will notice here that the rotation of the $(\text{H}_2\text{PC}_2\text{H}_4\text{PH}_2)\text{Pd}$ group and the formation of the Pd–C and Sn–C bonds synchronously occur, which is different from that of ethyne. In **9Esn**, the square of the Pd–Sn–C–C is not planar due to the twist of the activated ethene (see top view) because the activated ethene (ethane) takes the energetically favorable staggered conformation by the sp^3 orbital hybridization.

The energy barrier of the reaction (12.9 kcal/mol) is larger than that for the ethyne C≡C π bond activation (8.8 kcal/mol) as displayed in Figure 11, because the reaction from **8Esn** to **9Esn** is energetically almost neutral due to the destabilization of the product **9Esn**. A somewhat larger energy of 9.2 kcal/mol out of 12.9 kcal/mol is spent for the rotation of the $(\text{H}_2\text{PC}_2\text{H}_4\text{PH}_2)\text{Pd}$ group.

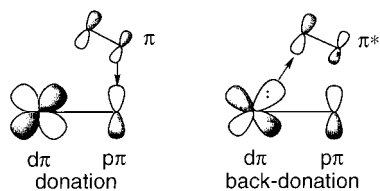
The activation of the C=O double bond with the lone pair electron at the Pd=Sn bond was also examined using a simple molecule, formaldehyde, giving the attention especially to the behavior of the phosphine ligand. In the reactant **8Fsn**, the incoming formaldehyde coordinates to the Sn by the donation of the lone pair electron on the oxygen to the p orbital of the

(22) The change in the distances of the Pd–C and Sn–C bonds from the transition state **TS4Gsn** (TS)⁹ to the product **9Gsn** (P)⁹ through point b (b) are as follows: the Pd–C bond, 2.214 Å (TS) → 2.064 Å (b) → 2.075 Å (P); the Sn–C bond, 2.533 Å (TS) → 2.118 Å (b) → 2.111 Å (P).

Sn with the O–Sn distance of 2.446 Å, where the H–C–H plane of the formaldehyde is parallel to the Pd–Sn–O plane while the $p\pi$ orbital of the C=O is perpendicular. No other structure with the η^2 -C=O coordination of formaldehyde to the Sn atom was found. The H–C–H plane of the coordinated formaldehyde becomes perpendicular to the Pd–Sn–O plane in the product **9Fsn** by its rotation with the formation of the Pd–C bond. It is of great interest that there are two pathways to produce **9Fsn** starting from **8Fsn**. One is accompanied by the rotation of the $(\text{H}_2\text{PC}_2\text{H}_4\text{PH}_2)\text{Pd}$ group around the Pd–Sn axis and another is not.

The coordination of the formaldehyde oxygen to the Sn atom by the electron donation enlarges the polarization of the $\text{C}(+\delta)=\text{O}(-\delta)$ π bond, and simultaneously enhances the nucleophilicity of the $d\pi$ orbital of the Pd with the large P–Pd–Sn angle of 141.4°. The positive charge of the carbon of the formaldehyde is increased to +0.179 e (+0.160 e for the free formaldehyde) and the Pd–P bond distance becomes longer when trans to the formaldehyde oxygen than when cis due to the localization of the electron on the $d\pi$ orbital of the Pd on the formaldehyde side by the electron flow along the C–O–Sn–Pd linkage. In contrast, in ethene and ethyne⁹ the Pd–P bond distance is shorter when trans to ethene or ethyne rather than when cis due to the different activation mechanism. As the reaction proceeds, the formaldehyde rotates to make the $p\pi$ orbital of the C=O parallel to the P–Pd–P plane, because the O–Sn distance is shortened and then both the nucleophilicity of the Pd $d\pi$ and the electrophilicity of the π orbital of the C=O carbon are furthermore enhanced. The rotation of the formaldehyde is completed by passing through the transition state **TS4Fsn1** with the formation of both the Pd–C and Sn–O bonds to form the product **9Fsn**. This activation reaction is obviously heterolytic, and is not accompanied by the rotation of the $(\text{H}_2\text{PC}_2\text{H}_4\text{PH}_2)\text{Pd}$ fragment around the Pd–Sn axis due to two reasons: (i) the C=O oxygen can strongly coordinate to the Sn atom without the rotation and (ii) the nucleophilicity of the Pd $d\pi$ is reduced by the rotation.

On the other hand, to reach another transition state **TS4Fsn2**, not only the coordinated formaldehyde but also the $(\text{H}_2\text{PC}_2\text{H}_4\text{PH}_2)\text{Pd}$ fragment rotates. It should be noted that the Pd–C distance is kept long, while the Sn–O distance is somewhat shortened by the electron donation from the C=O π orbital to the Sn p orbital as presented below at point a on the reaction coordinate (see Figure 13). In the transition state **TS4Fsn2**, the



Pd–C distance is shortened to 2.745 Å by the electron back-donation from the Pd $d\pi$ orbital to the C=O π^* orbital. One will notice here that this is homolytic C=O π bond activation with the rotation of the $(\text{H}_2\text{PC}_2\text{H}_4\text{PH}_2)\text{Pd}$ group around the Pd–Sn axis, which is similar to that of ethyne and ethene. The Pd–Sn–O–C plane is evidently twisted by the contribution of the lone pair electron of the C=O oxygen to stabilize the transition state, which is more strongly reflected on the structures at points b and c during the formation process of the Pd–C and the Sn–O

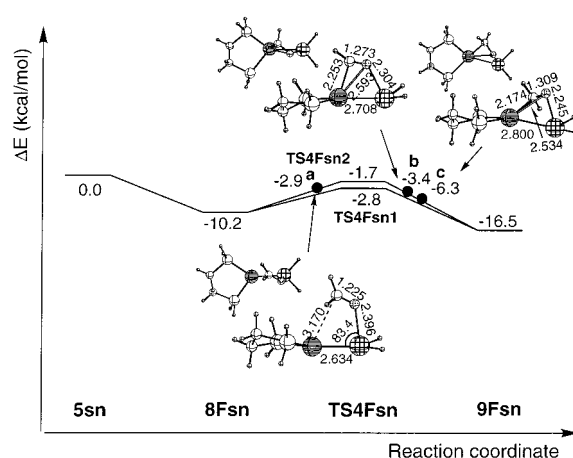


Figure 13. B3LYP/1 potential energy surfaces (in kcal/mol) of the activation of the C=O π bond of formaldehyde at the Pd=Sn bond of the $(\text{H}_2\text{PC}_2\text{H}_4\text{PH}_2)\text{Pd}=\text{SnH}_2$ complex **5sn**. The structures (in Å and deg) at points a, b, and c on the reaction coordinate are displayed together.

bonds with the further rotation of the $(\text{H}_2\text{PC}_2\text{H}_4\text{PH}_2)\text{Pd}$ group as presented in Figure 13.

Compared with the case of ethene, the intermediate **8Fsn**, the transition state **TS4Fsn2**, and the product **9Fsn** for the homolytic C=O π bond activation are stabilized by 5–10 kcal/mol due to the contribution of the lone pair electron of the C=O oxygen in the interaction between formaldehyde and $(\text{H}_2\text{PC}_2\text{H}_4\text{PH}_2)\text{Pd}=\text{Sn}$. The energy of 7.3 kcal/mol, which corresponds to 86% of the energy barrier, is needed to reach point a with the rotation of the $(\text{H}_2\text{PC}_2\text{H}_4\text{PH}_2)\text{Pd}$ group around the Pd–Sn axis just before the C=O π bond breaking. Although both transition states, **TS4Fsn1** for the heterolytic activation and **TS4Fsn2** for the homolytic activation, are lower in energy than **5sn**, the former was 1.1 kcal/mol more stable than the latter, indicating that the heterolytic activation is more facile than the homolytic one.

4. Concluding Remarks

The activation mechanism of the σ and π bonds at the Pd=X (X = Sn, Si, C) bonds of the model $(\text{H}_2\text{PC}_2\text{H}_4\text{PH}_2)\text{Pd}=\text{XH}_2$ complexes were theoretically investigated using a density functional method (B3LYP). The reaction mechanism significantly depends on the atom X, and the co-effect of the Pd–Sn combination successfully makes the reaction facile.

The O–H bond of H_2O is heterolytically activated at the Pd=X (X = Sn, Si) bonds without the rotation of the $(\text{H}_2\text{PC}_2\text{H}_4\text{PH}_2)\text{Pd}$ group around the Pd–Sn axis, the energy barrier being smaller for X = Si than for X = Sn. In contrast, at the Pd=C bond, the activation homolytically proceeds, depending on the electronic nature of the Pd=X bond. In all cases of X = Sn, Si, C, the activated O–H hydrogen forms a bond not with the X atom but with the Pd atom as the hydrido ligand. The mechanism of the activation of the C–H bond of CH_4 and the H–H bond of H_2 at the Pd=X (X = Sn, Si, C) bonds were similar to each other. The C–H and H–H bonds are heterolytically activated in all cases, and the hydrogen is extracted as a proton by the Pd atom in the case of X = Sn, Si and by the C atom in the case of X = C, since the nucleophile is switched between the Pd and the X atoms depending on the atom X. It is quite interesting that, for the O–H bond with the lone pair electron, the energy barrier is smaller for the heterolytic activation at the

Pd=Sn bond than for the well-known homolytic activation at the Pd of the $(\text{H}_2\text{PC}_2\text{H}_4\text{PH}_2)\text{Pd}$ fragment; this trend is completely reversed for the C–H and H–H bonds without the lone pair electron.

The π bond activation of the $\text{C}\equiv\text{C}$ triple bond of ethyne and the $\text{C}=\text{C}$ double bond of ethene at the Pd=Sn bond is accompanied by the rotation of the $(\text{H}_2\text{PC}_2\text{H}_4\text{PH}_2)\text{Pd}$ group around the Pd–Sn axis to successfully complete the reaction. The reaction is initiated by the coordination of the π bond via the η^2 mode to the Sn atom, and then the rotation of the $(\text{H}_2\text{PC}_2\text{H}_4\text{PH}_2)\text{Pd}$ group promotes both the electron donation from the π orbital to the Sn p orbital and the back-donation from the Pd $d\pi$ orbital to the π^* orbital. On the other hand, the activation of the $\text{C}=\text{O}$ π bond of formaldehyde with the lone pair electron at the Pd=Sn bond has two reaction pathways, both of them starting with the coordination of the formaldehyde oxygen to the Sn atom by the donation of the lone pair electron to the Sn p orbital. One is the homolytic activation with the rotation of the $(\text{H}_2\text{PC}_2\text{H}_4\text{PH}_2)\text{Pd}$ group, which is similar to the case of the $\text{C}\equiv\text{C}$ and $\text{C}=\text{C}$ π bond activations, and another is

the heterolytic one without the rotation of the $(\text{H}_2\text{PC}_2\text{H}_4\text{PH}_2)\text{-Pd}$ group as found for the water O–H bond activation. That is, this suggests that, during the homolytic activation of the π bond, the rotation of the $(\text{H}_2\text{PC}_2\text{H}_4\text{PH}_2)\text{Pd}$ group is necessary. Thus, the mechanism of the σ and π bond activation significantly depends on both the substrate and atom X, and the ligands XH_2 and phosphine play an important role in the mechanism of the present reaction.

Acknowledgment. The calculations were in part carried out at the Computer Center of the Institute for Molecular Science, Japan. T.M. was partly supported by the Grants-in-Aid from the Ministry of Education, Science, Sports, and Culture, Japan.

Supporting Information Available: Listings giving the optimized Cartesian coordinates of all equilibrium structures and transition states presented in this paper (PDF). This material is available free of charge via the Internet at <http://pubs.acs.org>.

JA0113495